

Synthesis of an intrinsically flame retardant bio-based benzoxazine resin

Hongqiang Yan ^{a,*}, Chuang Sun ^a, Zhengping Fang ^a, Xiaoqing Liu ^b, Jin Zhu ^b, Hao Wang ^c

^a Lab of Polymer Material and Engineering, Ningbo Institute of Technology, Zhejiang University, Ningbo, Zhejiang 315100, China

^b Ningbo Key Laboratory of Polymer Materials, Ningbo Institute of Materials Technology and Engineering, Chinese Academy of Sciences Institution, Ningbo, Zhejiang 315201, China

^c Centre of Excellence in Engineered Fibre Composites (CEEFC), University of Southern Queensland, Toowoomba, Queensland 4350, Australia

ARTICLE INFO

Keywords:

Diphenolic acid

Bio-based polymer

Benzoxazine

Intrinsically flame retardant

Synthesis

ABSTRACT

An intrinsically flame retardant bio-based benzoxazine (diphenolic acid pentaerythritol caged phosphate benzoxazine, DPA-PEPA-Boz) monomer was synthesized from bio-based diphenolic acid (DPA) using a four-step process. The monomer of DPA-PEPA-Boz was characterized by FT-IR, ¹H NMR and ¹³C NMR. The curing behavior of DPA-PEPA-boz was studied and compared with those of DPA based benzoxazine (DPA-Boz) and DPA ester derivative (MDP) based benzoxazine (MDP-Boz) without PEPA by means of non-isothermal differential scanning calorimetry. The results indicated that DPA-PEPA-Boz system showed a two-stage curing, assigned to the exothermic opening reactions of oxazine rings and P–O–C ring in PEPA respectively, while the DPA-Boz and MDP-Boz showed a one-stage curing. In addition, the effect of the introduction of PEPA on thermal and inflammable properties of the resin was evaluated. The residual char of the cured DPA-PEPA-Boz (P-DPA-PEPA-Boz) after 400 °C was much higher than those of cured DPA-Boz (P-DPA-Boz) and cured MDP-Boz (P-MDP-Boz) under nitrogen and air atmospheres. Meanwhile, total heat release (THR), peak heat release rate (PHRR) and heat release capacity (HRC) of P-DPA-PEPA-Boz were about half of those of P-DPA-Boz and P-MDP-Boz. P-DPA-PEPA-Boz had a limiting oxygen index (LOI) of 33.5% and achieved V0 rating in UL94 test. P-DPA-PEPA-Boz behaved as a very good intrinsic thermal and flame retardant bio-based benzoxazine resin.

1. Introduction

The development of environmentally friendly polymers from bio-based materials and compounds is one of the current challenges and also opportunities for polymer chemistry. Many new bio-based compounds have been developed and commercialized for the production of bio-based polymers, which have the potential of significant economic and environmental benefits to the society and creating new property profiles that the traditional non-renewable polymers do not exhibit [1,2]. Up to now, much effort has been made to synthesize polylactic acid, polycarbonates, polyesters, epoxy resin and benzoxazine resin from renewable feedstock, such as rosin, cyclodextrins, soybean oil, diphenolic acid, itaconic acid, etc [3–10].

Benzoxazine resins (Bozs) have attracted increasing attention in

the past decade due to their excellent high temperature stability, low water absorption, good dielectric properties and structure-design flexibility, in addition to their zero shrinkage or a slight expansion upon curing [11–14]. These good properties give them a huge potential in industrial applications, such as high-speed printed circuit boards, aerospace structural composites, etc [15–19]. The bisphenol A (BPA) based Boz (BPA-Boz) stands out from many types of Bozs due to its high structural integrity and superior properties [20]. Diphenolic acid (DPA), which has a structure similar to BPA (Fig. 1), can be prepared from low-grade lignin and cellulose biomass resources [21]. Through plant photosynthesis to synthesize cellulose, it is a renewable material that can alleviate our current large dependence on petroleum for chemicals, preserve the planet nature resources, and obtain good environmental and economic benefits [22]. DPA is commercially available and much cheaper than BPA and has the ability to introduce functional carboxyl group into the polymer structure. Therefore DPA is believed to be a cheap bio-based compound in large scale and can be used as a BPA alternative to synthesize new polymers. In the last

* Corresponding author.

E-mail address: yanhongqiang@nit.net.cn (H. Yan).

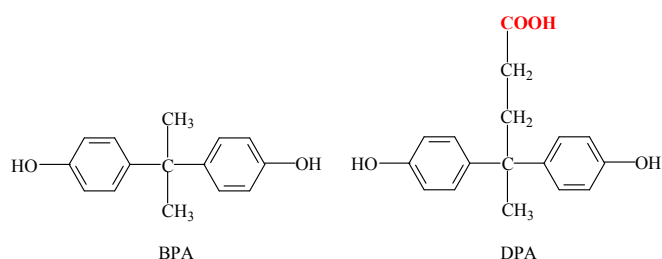


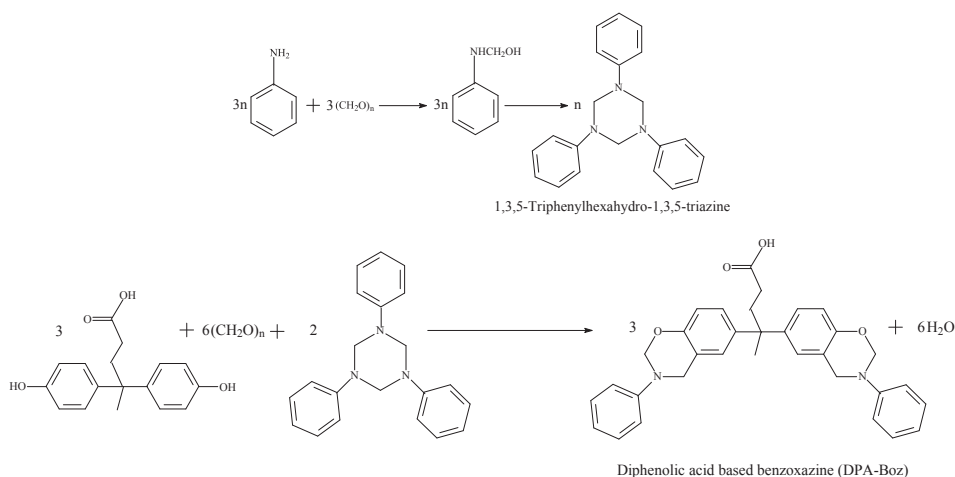
Fig. 1. The structure comparison between BPA and DPA.

decade, DPA has attracted much attention from researchers to replace BPA for synthesizing new polyesters, polycarbonates and Bozs [7,23–27].

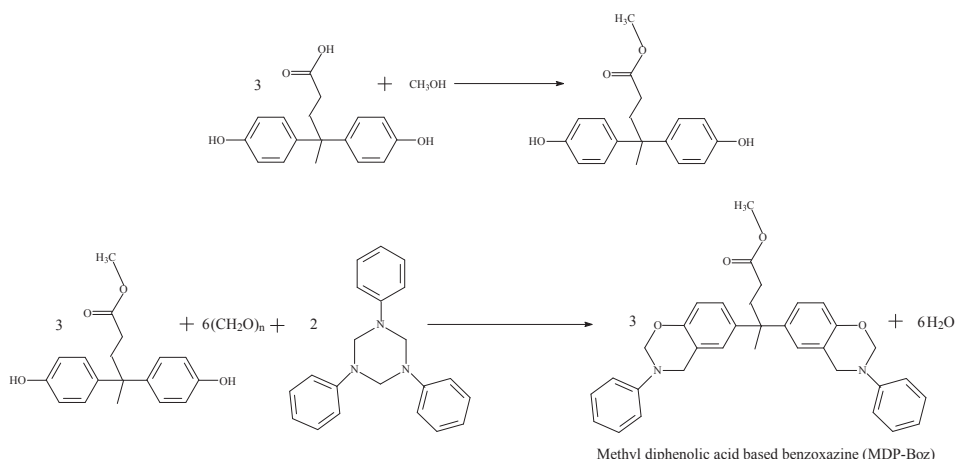
With the rapid development of aerospace, microelectronics and energy industries, there is an urgent requirement to further improve the properties of Bozs, such as heat resistance, flame retardancy, toughness, low dielectric constant, *etc* [28]. The flame retardancy of BPA-Boz cannot meet the more demanding requirement. Challenges also exist for the diphenolic acid based Boz (DPA-boz) in this regard. For example, DPA-Boz has been modified using DOPO or DOPO-2Me to prepare Boz foams [27]. But the choice of flame retardant is limited due to the poor compatibility between

flame retardant and Boz. Fortunately, with the carboxyl group in the DPA-boz structure, it is possible to introduce flame retardant moieties to improve its flame retardancy. Common flame retardants contain N, P, Si and halogen elements. Researchers pay more attention to P containing flame retardants because of their better flame retardant effect, less smoke, and lower emissions of harmful substances. A representative P containing flame retardant is 4-(hydroxymethyl)-1-oxido-2,6,7-trioxo-1-phosphabicyclo [2.2.2]octane (PEPA), which was synthesized by Verkade for the first time in the 1960s [29]. It has aroused people's great interest due to the highly symmetrical cage structure in its molecule. PEPA can be used as intumescent type flame retardant because its molecule contains acid source and carbonization agent, which resulting in characteristics of good char-forming ability and excellent thermal stability. Synthesis of cage phosphate ester compounds and their application in flame retardant materials have received wide attention in recent years [30–33].

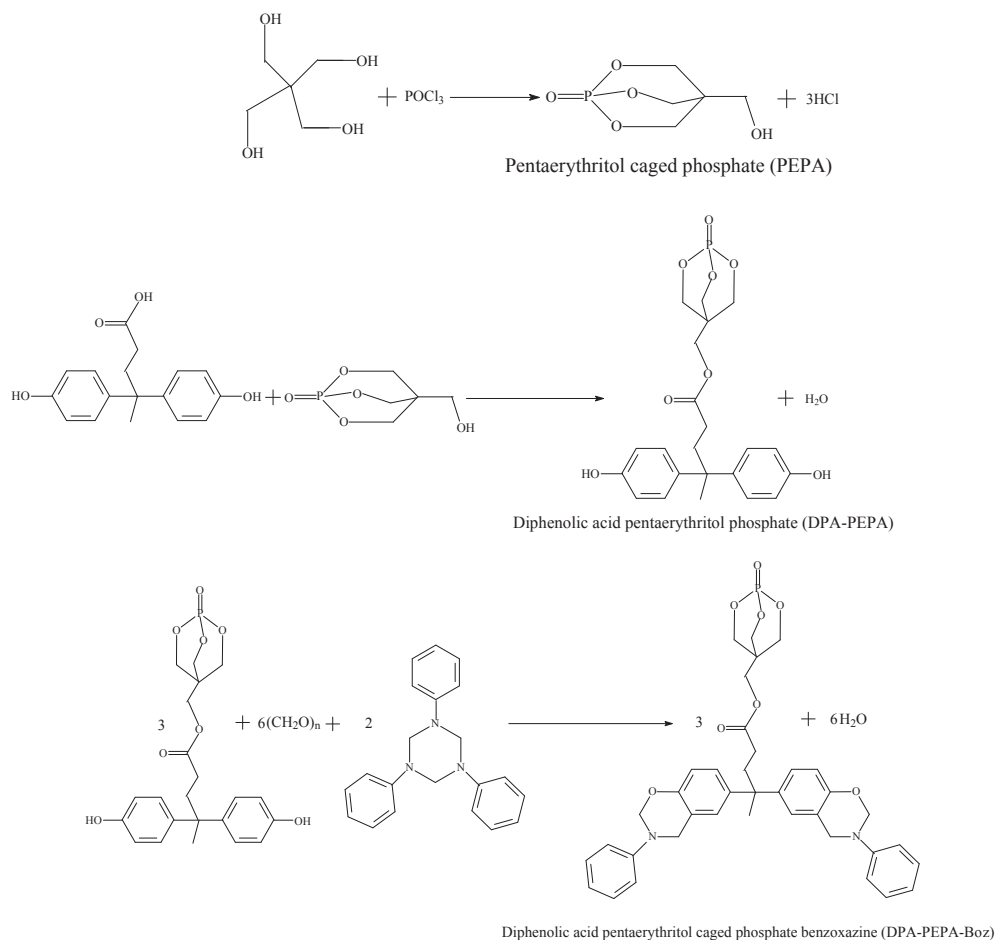
In this study, an intrinsically flame retardant bio-based Boz (DPA-PEPA-boz) was synthesized from renewable diphenolic acid. The material was characterized by fourier transform infrared (FTIR) spectrophotometer, ^1H and ^{13}C nuclear magnetic resonance (NMR). Its curing behavior, thermal and inflammable properties were evaluated and compared with DPA based Boz (DPA-boz) and DPA ester derivative (MDP) based Boz (MDP-boz).



Scheme 1. Schematic pathway of synthesis of DPA-Boz.



Scheme 2. Schematic pathway of synthesis of MDP-Boz.



Scheme 3. Schematic pathway of synthesis of DPA-PEPA-Boz.

2. Experimental

2.1. Materials

The following chemicals were analytical purity, obtained from Aladdin Industrial Corporation: diphenolic acid (98%), para-formaldehyde (95%), aniline (99.5%), pentaerythritol (98%), *p*-toluene sulfonic acid (99%), toluene (99%), phosphorus oxychloride (98%), ethyl acetate (99.5%), petroleum ether (boiling range: 60–90 °C), sodium sulfate (99%), sodium hydrogen carbonate (99%), sodium chloride (99.5%), acetonitrile (99%), chloroform (99%), sodium hydroxide (96%), hydrochloric acid (38%), diethyl ether (99.5%), hexane (95%), 1,4-dioxane (99.5%), methanol (99.5%). All solvents were purified by standard procedures.

2.2. Synthesis of DPA-Boz monomer

The synthesis pathway of DPA-Boz was as follows (Scheme 1):

2.2.1. Synthesis of 1,3,5-triphenylhexahydro-1,3,5-triazine [34]

Paraformaldehyde (0.02 mol) and aniline (0.01 mol) were mixed for 35 min at 70 °C. The product was dissolved in chloroform, washed with a 1 mol/L sodium hydroxide aqueous solution and recrystallized from diethyl ether. White crystals were obtained with a yield of 70.2%. Characterization of the crystal was summarized as follows:

IR (ν/cm^{-1}): 1599, 1499, 755 and 689 (monosubstituted benzene, ν); 1334 (C–N–C, as); 1203 (C–N–C, s); 1163 (C–N–C, γ).

^1H NMR (ppm, CDCl_3): 4.88 (d, N–CH₂–N, 6H); 6.76, 7.06 and 7.16 (q, –Ar–H, 15H).

^{13}C NMR (ppm, CDCl_3): 67.35 (–N–CH₂–N–, 3C); 120.58, 129.60, 117.52 and 149.0 (–N–Ar, 18C).

2.2.2. Synthesis of DPA-Boz monomer [35]

1,3,5-Triphenylhexahydro-1,3,5-triazine (0.02 mol), para-formaldehyde (0.083 mol), diphenolic acid (0.03 mol) and 150 mL of toluene were placed into 500 mL three-necked round-bottom flask. The reaction mixture was heated at 110 °C for 6 h. The resulting light orange solution was filtered and concentrated at reduced pressure to obtain yellow syrup. Finally, the yellow syrup was subsequently dried in a vacuum oven giving a yellowish solid of DPA-Boz with a yield of 94.8%. Characterization of DPA-boz was summarized as follows:

IR (ν/cm^{-1}): 3435, 1452 (–OH, ν); 1705 (C=O, ν); 1257 (C–O, ν); 1234, 1165 (C–O–C, ν); 943 (C–H of oxazine ring, γ); 1496 (1,2,4-trisubstituted benzene, ν).

^1H NMR (ppm, CDCl_3): 7.30–6.70 (t, Ar–H, 16H); 5.34 (s, O–CH₂–N, 4H); 4.58 (s, Ar–CH₂–N, 4H); 2.35 (t, –C–CH₂–CH₂–CO–, 2H); 2.13 (t, –C–CH₂–CH₂–CO–, 2H); 1.53 (s, –CH₃, 3H).

^{13}C NMR (ppm, CDCl_3): 179.9 (–CO–, 1C); 152.5, 141.1, 126.9, 125.3, 120.4 and 116.7 (–C–Ar–O–, 12C); 148.5, 129.4, 121.4 and 118.1 (–N–Ar, 12C); 79.2 (–O–C–N–, 2C); 50.7 (–Ar–C–N–Ar, 2C); 44.6 (CH₃–C–, 1C); 36.4 (–C–CH₂–CH₂–CO–O–, 1C); 30.2 (–C–CH₂–CH₂–CO–O–, 1C); 27.8 (–CH₃, 1C).

2.3. Synthesis of MDP-Boz monomer

The synthesis pathway of MDP-Boz was as follows (Scheme 2):

2.3.1. Synthesis of methyl diphenolic acid (MDP) [35]

A 500 mL round-bottom flask equipped with a condenser was charged with diphenolic acid (0.13 mol), *p*-toluenesulfonic acid monohydrate (2×10^{-2} mol), trimethyl orthoformate (0.19 mol) and 100 mL of methanol. The mixture was refluxed for 16 h, then the methanol was removed at reduced pressure. The resulting syrup was dissolved in ethyl ether and washed three times with a NaHCO_3 saturated solution and with water respectively. Finally, the ethyl ether was removed with a rotary evaporator and the product was dried at reduced pressure and room temperature. The resulting product of MDP was milled and used without further purification in the next step. A yield of 88% was obtained. Characterization of MDP was summarized as follows:

IR (v/cm^{-1}): 3385 ($-\text{Ar}-\text{OH}$, s); 2956 ($-\text{CH}_3$ and $-\text{CH}_2-$, s); 1703 ($\text{C}=\text{O}$, v); 1608 ($-\text{Ar}-\text{H}$, s); 1220 ($\text{C}-\text{O}-\text{C}$, v); 1450.5 ($-\text{CH}_2-$, v); 1386.2 ($-\text{CH}_3$, v);

^1H NMR (ppm, DMSO): 9.23(t, $\text{Ar}-\text{OH}$, 2H); 6.91(t, $-\text{Ar}-\text{H}$, 4H); 6.71(t, $-\text{Ar}-\text{H}$, 4H); 3.61(t, $-\text{CO}-\text{O}-\text{CH}_3$, 3H); 2.25 (t, $-\text{C}-\text{CH}_2-\text{CH}_2-\text{CO}-$, 2H); 2.11(t, $-\text{C}-\text{CH}_2-\text{CH}_2-\text{CO}-$, 2H); 1.5 (s, $-\text{C}-\text{CH}_3$, 3H).

2.3.2. Synthesis of MDP-Boz monomer [35]

A 250 ml 3-necked round-bottom flask equipped with a magnetic stirrer and a condenser was charged with 1,3,5-triphenylhexahydro-1,3,5-triazine (0.02 mol), paraformaldehyde (0.08 mol), MDP (0.03 mol) and 120 mL of toluene. The mixture was refluxed at 110°C for 20 h. After cooling to room temperature, MDP-boz monomer was filtered, dissolved in ethyl ether, and washed five times with a 3 mol/L sodium hydroxide solution and with water respectively. After washing, the organic phase was dried over sodium sulfate and the solvent was evaporated at reduced pressure and room temperature. A pale yellowish solid of MPD-Boz was obtained with a yield of 92.2%. Characterization of MDP-boz was summarized as follows:

IR (v/cm^{-1}): 1734 ($\text{C}=\text{O}$, v); 1234, 1030 ($\text{C}-\text{O}-\text{C}$, v); 945 ($\text{C}-\text{H}$ of oxazine ring, γ); 1496 (1,2,4-trisubstituted benzene, v); 1368 ($-\text{CH}_3$, v) 1456.5 ($-\text{CH}_2-$, v).

^1H NMR (ppm, DMSO): 7.32–6.74 (t, $\text{Ar}-\text{H}$, 16H); 5.37 (s, $\text{O}-\text{CH}_2-\text{N}$, 4H); 4.62 (s, $\text{Ar}-\text{CH}_2-\text{N}$, 4H); 3.63 (t, $-\text{CO}-\text{O}-\text{CH}_3$, 3H);

2.40 (t, $-\text{C}-\text{CH}_2-\text{CH}_2-\text{CO}-$, 2H); 2.14 (t, $-\text{C}-\text{CH}_2-\text{CH}_2-\text{CO}-$, 2H); 1.56 (s, $-\text{CH}_3$, 3H).

^{13}C NMR (ppm, DMSO): 174.4 ($-\text{CO}-$, 1C); 152.5, 141.2, 126.9, 125.3, 120.3 and 116.6 ($-\text{C}-\text{Ar}-\text{O}-$, 12C); 148.5, 129.3, 121.3 and 118.0 ($-\text{N}-\text{Ar}$, 12C); 79.2 ($-\text{O}-\text{C}-\text{N}-$, 2C); 51.7 ($-\text{Ar}-\text{C}-\text{N}-\text{Ar}$, 2C); 50.7 ($-\text{CO}-\text{O}-\text{CH}_3$); 44.6 ($-\text{C}-\text{CH}_3$, 1C); 36.6 ($-\text{C}-\text{CH}_2-\text{CH}_2-\text{CO}-\text{O}-$, 1C); 30.1 ($-\text{C}-\text{CH}_2-\text{CH}_2-\text{CO}-\text{O}-$, 1C); 27.8 ($-\text{C}-\text{CH}_3$, 1C);

2.4. Synthesis of DPA-PEPA-Boz monomer

The synthesis pathway of diphenolic acid pentaerythritol caged phosphate benzoxazine (DPA-PEPA-Boz) was as follows (Scheme 3):

2.4.1. Synthesis of pentaerythritol caged phosphate (PEPA) [29]

Pentaerythritol (PEA) (0.25 mol) and 1,4-dioxane (80 ml) were placed into a 250 ml four-necked round-bottom flask equipped with a magnetic stirring device, a condensation reflux device, a thermometer and a constant pressure feeding hopper. 1 mol/L sodium hydroxide aqueous solution was used to absorb the exhaust gas. Under a flow of N_2 , phosphorus oxychloride was put into the constant pressure feeding hopper, adjusting the cock to make sure the phosphorus oxychloride gradually dripped into the flask within 2 h. Then the mixture was refluxed for 5 h, cooled gradually to room temperature and filtered out the white precipitate. The white precipitate was washed once with 100 ml 1,4-dioxane followed by twice with 200 ml hexane, and then dried in a vacuum oven at 80°C . Then white powder (PEPA) was obtained at a yield about 87.6%. Characterization of the PEPA was summarized as follows:

IR (v/cm^{-1}): 1299 ($\text{P}=\text{O}$, v); 1025 ($\text{P}-\text{O}-\text{C}$, v); 1152 ($\text{C}(\text{CH}_2)_4-$, v); 959 ($-\text{CH}_2-\text{OH}$, v); 876, 767, 669 and 632 ($-\text{P}-\text{O}-\text{C}$, v); 2963 ($-\text{CH}_2-$, v); 2910 ($-\text{CH}_2-$, γ).

^1H NMR (ppm, DMSO): 5.1 (s, $-\text{OH}$, 1H); 3.31 (s, $-\text{C}-\text{CH}_2-\text{OH}$, 2H); 4.52 (d, $-\text{P}-\text{O}-\text{CH}_2-\text{C}$, 6H).

^{13}C NMR (ppm, DMSO): 77.1 ($-\text{O}-\text{CH}-\text{C}$, 3C); 58.4 ($\text{C}(\text{CH}_2)_4-$, 1C); 39.4 ($-\text{CH}_2-\text{OH}$, 1C).

^{31}P NMR (ppm, DMSO): -7.02 .

2.4.2. Synthesis of diphenolic acid pentaerythritol phosphate (DPA-PEPA)

Diphenolic acid (DPA) (0.05 mol), PEPA (0.1 mol), *p*-toluene sulfonic acid (2.86 g) and 120 ml acetonitrile were placed into a 250 ml three-necked round-bottom flask equipped with a magnetic stirring device, a condensation reflux device and a thermometer. Under a flow of N_2 , the mixture was heated at 70°C for 24 h and evaporated through the rotary evaporation to obtain a pink powder. The pink powder was dissolved in ethyl acetate, then washed three times with saturated sodium hydrogen carbonate solution and saturated sodium chloride solution respectively. The products dissolved in ethyl acetate were separated by the chromatographic column. The selected expansion agent used was a mixture of ethyl acetate and petroleum ether (volume 3:1). A white powder (DPA-PEPA) was obtained after drying in a vacuum dryer at 40°C , and its yield was 80.2%. Characterization of the DPA-PEPA was summarized as follows:

IR (v/cm^{-1}): 1735 ($\text{C}=\text{O}$, v); 1261 ($\text{C}-\text{O}-\text{C}$, as); 1157 ($\text{C}(\text{CH}_2)_4-$, v); 2956 ($-\text{CH}_2-$, s); 3376 ($-\text{OH}$, v); 863, 838, 672, 577 ($-\text{P}-\text{O}-\text{C}-$, v).

^1H NMR (ppm, DMSO): 9.22 (s, $-\text{Ar}-\text{OH}$, 2H); 6.96 and 6.67 (d, $-\text{Ar}-\text{H}$, 8H); 4.63 (s, $-\text{P}-\text{O}-\text{CH}_2-\text{C}$, 6H); 3.91 (d, $-\text{CO}-\text{O}-\text{CH}_2-\text{C}$, 2H); 2.25 (t, $-\text{CH}_2-\text{CH}_2-\text{CO}$, 2H); 2.09 (t, $-\text{C}-\text{CH}_2-\text{CH}_2-$, 2H); 1.46 (s, $-\text{CH}_3$, 3H).

^{13}C NMR (ppm, DMSO): 172.9 ($-\text{C}-\text{CO}-\text{O}-$, 1C); 155.2, 138.9, 127.6 and 115.5 ($\text{HO}-\text{Ar}$, 12C); 75.8 ($-\text{C}-\text{CH}_2-\text{O}-\text{P}-$, 3C); 59.5 ($-\text{CO}-\text{O}-\text{CH}_2-\text{C}$, 1C); 43.5 (CH_3-C , 1C); 36.9

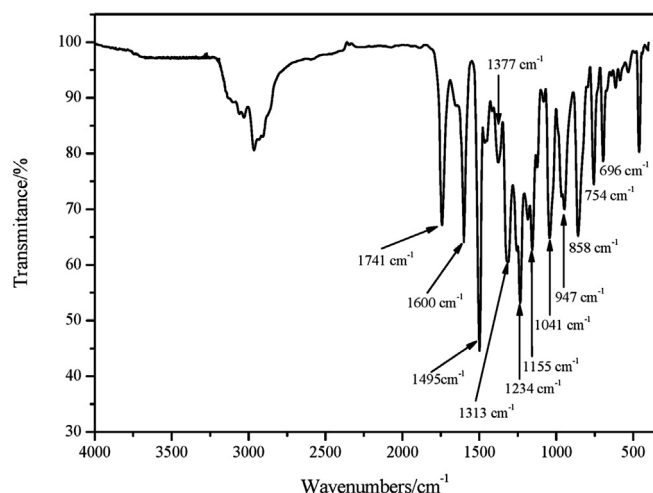


Fig. 2. The FTIR spectrum of DPA-PEPA-Boz.

Table 1
The characteristic absorption wavenumbers in FTIR spectrum of DPA-PEPA-Boz.

Chemical group	Absorption wavenumbers/cm ⁻¹
–P–O–C–C–P ring	858, 754, 696
Out-of-plane C–H	947
C–(CH ₂) ₄ –	1155
C–O–C	1234, 1041
–P=O	1313
C–N–C	1377
1,2,4-trisubstituted benzene	1498
Alkene C=C stretching bands	1600
–C=O	1741

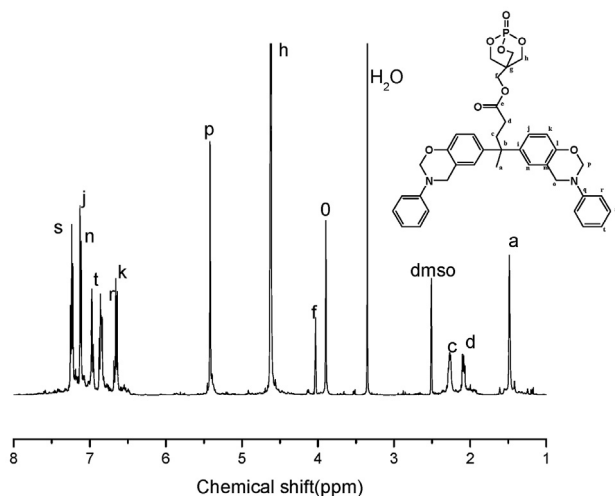


Fig. 3. ¹H NMR spectrum of DPA-PEPA-Boz.

(–CH₂–CH₂–CO–O–, 1C); 35.9 (–CO–O–CH₂–C–CH₂–, 1C); 29.5 (–C–CH₂–CH₂–CO–, 1C); 27.1 (–C–CH₃, 1C).

2.4.3. Synthesis of diphenolic acid pentaerythritol caged phosphate Boz (DPA-PEPA-Boz)

A 250 ml three-necked round-bottom flask equipped with a magnetic stirrer and a condenser was charged with 1,3,5-

triphenylhexahydro-1,3,5-triazine (0.005 mol), paraformaldehyde (0.018 mol), DPA-PEPA (0.0075 mol) and 120 ml toluene. Under a flow of N₂, the mixture was refluxed for 20 h. After cooling to room temperature, the Boz monomer was filtered, dissolved in ethyl ether and washed five times with 3 mol/L sodium hydroxide aqueous solution. Then the organic phase was dried over sodium sulfate and the solvent was evaporated at reduced pressure and room temperature. A light yellow powder (DPA-PEPA-boz) was obtained with a yield of 85.7%. Characterization of the DPA-PEPA-Boz was summarized as follows:

IR (v/cm⁻¹): 1741 (C=O, v); 1234, 1041 (C–O–C, v); 1313 (P=O, v); 1155 (C–(CH₂)₄–, v); 858, 754, 696 (P–O–C–C–P, v); 947 (C–H of oxazine ring, γ); 1498 (1,2,4-trisubstituted benzene, v).

¹H NMR (ppm, DMSO): 7.25–6.64 (t, Ar–H, 16H); 5.42 (s, O–CH₂–N, 4H); 3.89 (s, Ar–CH₂–N, 4H); 4.62 (t, –P–O–CH₂–C, 6H); 4.03 (t, –CO–O–CH₂–C, 2H); 2.26 (t, –C–CH₂–CH₂–CO–, 2H); 2.09 (t, –C–CH₂–CH₂–CO–, 2H); 1.48 (s, –CH₃, 3H).

¹³C NMR (ppm, DMSO): 174.7 (–CO–, 1C); 151.8, 140.7, 129.1, 128.9, 126.4 and 120.3 (–C–Ar–O–, 12C); 147.8, 137.4, 125.1 and 117.4 (–N–Ar, 12C); 115.8 (–O–C–N–, 2C); 78.4 (–C–CH₂–O–P–, 3C); 76.3 (–CO–O–CH₂–C–, 1C); 57.7 (–Ar–C–N–Ar, 2C); 49.2 (CH₃–C–, 1C); 44.1 (–C–CH₂–CH₂–CO–O–, 1C); 36.2 (C(CH₂)₄–, 1C); 29.8 (–CH₃, 1C); 27.0 (–C–CH₂–CH₂–CO–O–, 1C).

2.5. Preparation of benzoxazine resins

A certain amount of DPA-Boz, MDP-Boz and DPA-PEPA-Boz were taken respectively into three beakers and heated in a vacuum oven at 110 °C until a transparent melt without bubbles was formed. Then the melt was transferred to the PTFE mold (100 × 6 × 3 mm³ mold for limiting oxygen index (LOI) tests and 130 × 13 × 3 mm³ mold for vertical burning tests) and placed in an oven at 110 °C. The curing procedures was designed as 120 °C/1 h, 140 °C/1 h, 160 °C/1 h, 180 °C/1 h, 200 °C/1 h, 220 °C/1 h and 240 °C/1 h.

2.6. Monomer and resin characterization

FTIR test of the synthesized monomers were carried out on a Nexus 470-Thermo FTIR spectrophotometer in the range of 400–4000 cm⁻¹ using solid KBr pellet.

¹H NMR, ¹³C NMR and ³¹P NMR of the synthesized compounds were conducted on a BRUKER-Advance 2B (500 MHz) spectrometer

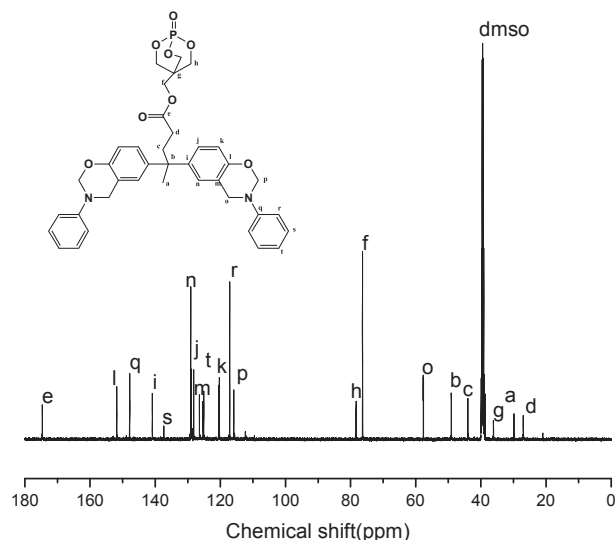


Fig. 4. ¹³C NMR spectrum of DPA-PEPA-Boz.

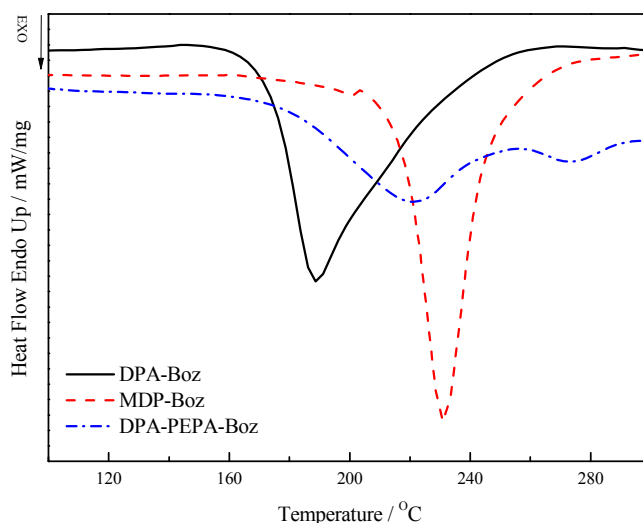


Fig. 5. DSC curves of DPA-Boz, MDP-Boz and DPA-PEPA-Boz.

Table 2
Parameters relating to the curing behavior of DPA-Boz, MDP-Boz and DPA-PEPA-Boz.

Sample	$T_{onset}/^{\circ}\text{C}$	$T_{max1}/^{\circ}\text{C}$	$T_{max2}/^{\circ}\text{C}$	$T_{offset}/^{\circ}\text{C}$	$\Delta H/\text{J/g}$
DPA-Boz	151.7	189.2	—	267.2	323.7
MDP-Boz	166.5	230.6	—	280.5	353.9
DPA-PEPA-Boz	159.3	221.7	272.0	293.7	115.4

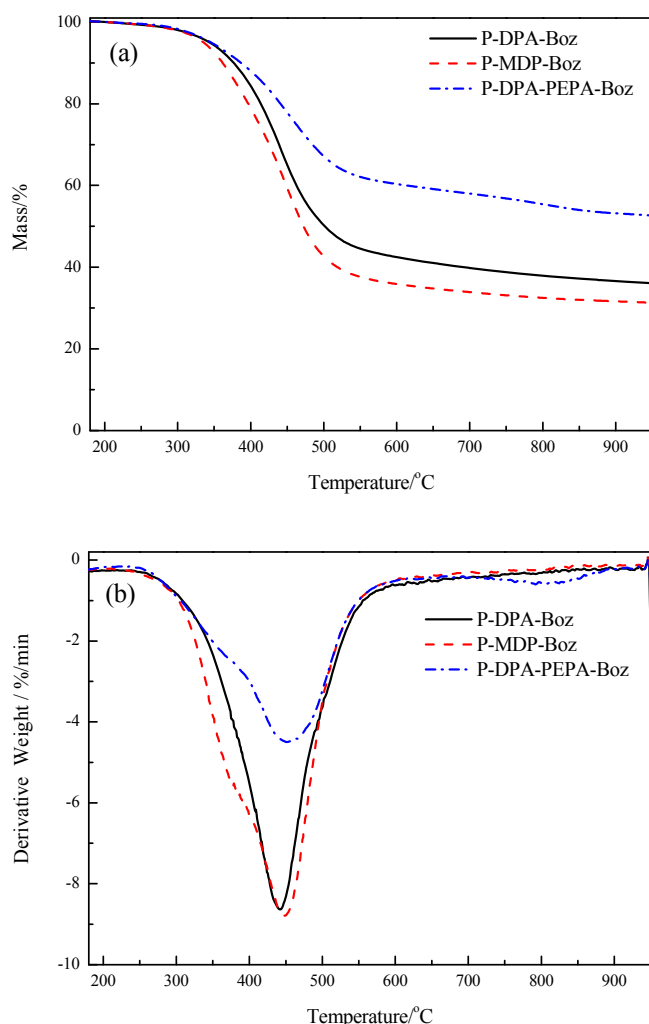


Fig. 6. TG curves of the cured benzoxazine resins from DPA-Boz, MDP-Boz and DPA-PEPA-Boz under nitrogen atmosphere, (a) TG curves and (b) DTG curves.

at room temperature using CDCl_3 or DMSO as solvent.

Differential scanning calorimetry (DSC) measurements were performed with a Netzsch 200 P C supported with a Netzsch TASC 414-5 computer for data acquisition. DSC was calibrated with high purity indium, and the measurements were conducted under a nitrogen flow of $20 \text{ cm}^3/\text{min}$. In DSC experiments, all the samples were subjected to a dynamic DSC scanning from 50 to $300 ^{\circ}\text{C}$ at a heating rate of $10 ^{\circ}\text{C}/\text{min}$.

Thermogravimetric (TG) analysis was carried out using a TGA 209 F1 Thermal Analyzer (Netzsch, Germany) to study the thermal degradation behavior of the cured resins. Samples were heated from room temperature to $950 ^{\circ}\text{C}$ at a heating rate of $20 ^{\circ}\text{C}/\text{min}$ under nitrogen with a flow rate of $40 \text{ cm}^3/\text{min}$ or air with a flow rate of $50 \text{ cm}^3/\text{min}$.

X-Ray photoelectron spectroscopy (XPS) spectra of P-DPA-PEPA-bozs, along with the char residues after keeping at $450 ^{\circ}\text{C}$ in a

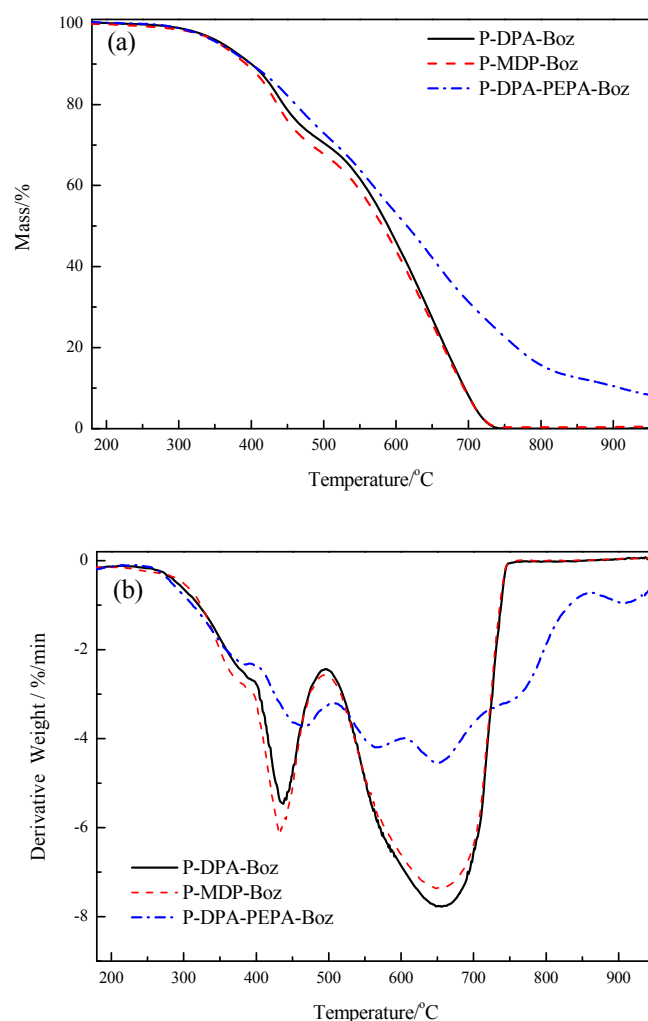


Fig. 7. TG curves of cured benzoxazines from DPA-Boz, MDP-Boz and DPA-PEPA-Boz under air atmosphere, (a) TG curves and (b) DTG curves.

muffle for 5 min, were obtained on a Thermo ESCALAB 250 spectrometer.

Microscale combustibility experiments were conducted using an MCC-2 microscale combustibility calorimeter (Govmark, USA). 5 mg sample was heated to $750 ^{\circ}\text{C}$ at a heating rate of $1 ^{\circ}\text{C}/\text{s}$ in a mixed stream of oxygen and nitrogen flowing at 20 and $80 \text{ cm}^3/\text{min}$ respectively.

Limiting oxygen index (LOI) was measured by using an HC-2 Oxygen Index Instrument (Jiangning Analytical Instrument Co. Ltd., Nanjing, China) on testing specimens ($100 \times 6 \times 3 \text{ mm}$) according to ASTM D2863-2008 procedure.

Vertical burning tests were performed with a CZF-3 Vertical Burning Tester (Jiangning Analytical Instrument Co. Ltd., Nanjing, China) on testing specimens ($130 \times 13 \times 3 \text{ mm}^3$) according to ASTM D3801 standard.

3. Results and discussion

3.1. Determination of the structure of DPA-PEPA-Boz monomer

The bio-based Boz monomer (DPA-PEPA-boz) was synthesized using a three-step process as shown in Scheme 3. First, pentaerythritol caged phosphate (PEPA) was obtained by treating pentaerythritol with phosphorus oxychloride. The yield was 87.6%. Second,

Table 3

TG results of the cured benzoxazine resins from DPA-Boz, MDP-Boz and DPA-PEPA-Boz under nitrogen atmosphere.

Sample	Temperature (°C)				Peak value (wt%/min)	Char (%)
	$T_{5\%}$	$T_{10\%}$	T_{max}	$T_{50\%}$		
P-DPA-Boz	343.6	376.6	442.2	501.2	-8.64	37.9
P-MDP-Boz	335.3	361.3	448.4	479.3	-8.79	32.5
P-DPA-PEPA-Boz	341.5	385.4	452.0	>950	-4.50	55.4

 $T_{5\%}$, $T_{10\%}$ and $T_{50\%}$ are the temperatures for 5%, 10% and 50% mass losses, respectively.**Table 4**

TG results of cured benzoxazines from DPA-Boz, MDP-Boz and DPA-PEPA-Boz under air atmosphere.

Sample	Temperature (°C)					Peak value ₁ (wt%/min)	Peak value ₂ (wt%/min)	$T_{Char=0}$ (°C)
	$T_{5\%}$	$T_{10\%}$	T_{max1}	T_{max2}	$T_{50\%}$			
P-DPA-Boz	360.3	400.3	437.1	656.0	589.3	-5.46	-7.78	747.4
P-MDP-Boz	355.7	392.7	433.1	648.2	581.7	-6.16	-7.37	746.2
^a P-DPA-PEPA-Boz	355.5	399.5	—	—	615.5	—	—	>950

^a The DTG curve of P-DPA-PEPA-Boz showed a four-stage weight loss process. Their T_{max} s were 467.0, 569.0, 650.0 and 744.0 °C respectively, and their Peak values were -3.73, -4.20, -4.54 and -3.20 wt%/min respectively.

the diphenolic acid (DPA) was reacted with PEPA in acetonitrile at 70 °C to obtain diphenolic acid pentaerythritol caged phosphate (DPA-PEPA), and its yield was 80.2%. Finally, DPA-PEPA-Boz was obtained by the reaction among 1,3,5-triphenylhexahydro-1,3,5-triazine, DPA-PEPA and paraformaldehyde in toluene at 110 °C for 20 h. The yield of DPA-PEPA-Boz was 85.7%.

The infrared spectrum of DPA-PEPA-Boz was shown in Fig. 2. The characteristic absorption wavenumbers in FTIR spectrum were listed in Table 1. As shown in Fig. 2 and Table 1, the presence of cyclic ether in the benzoxazine structure was confirmed by the absorbance peaks at about 1234 and 1041 cm^{-1} due to the symmetric stretching and asymmetric stretching modes of the C—O—C band of oxazine ring respectively. There was an obvious characteristic peak of out-of-plane C—H of oxazine ring at 947 cm^{-1} . The characteristic band at 1377 cm^{-1} was assigned to the asymmetric stretching vibrations of C—N—C bond of oxazine ring. There were characteristic bands at 858, 754 and 696 cm^{-1} assigned to the symmetric stretching and asymmetric stretching modes of -P-O-C-ring. The characteristic bands at 1313 cm^{-1} and 1155 cm^{-1} were assigned to the symmetric stretching modes of -P=O and C-(CH₂)₄- respectively. These results could confirm the oxazine ring and PEPA in the structure of DPA-PEPA-Boz.

The ¹H NMR spectrum of DPA-PEPA-Boz was shown in Fig. 3. The DPA-PEPA-Boz exhibited not only the specific signals of the oxazine ring, but also the chemical shifts that belong to PEPA. The two signals at 5.42 ppm (s, 4H) and 3.89 ppm (s, 4H) were corresponded to -O-CH₂-N and -Ar-CH₂-N- protons of oxazine ring respectively. Methyl protons of the DPA appeared at 1.48 ppm (s, 3H). Methylene protons of the DPA appeared at 2.26 ppm (t, -C-CH₂-CH₂-CO-, 2H) and 2.09 ppm (t, -C-CH₂-CH₂-CO-, 2H) respectively, while the two signals of methylene protons from PEPA were at 4.62 ppm (t, -P-O-CH₂-C, 2H) and 4.03 ppm (t, -O-CH₂-C, 2H) respectively. Moreover, integration analysis of the oxazine and aromatic proton peaks pointed out that the closed-ring structured monomer was about 98%.

The ¹³C NMR spectrum of DPA-PEPA-Boz was shown in Fig. 4. The corresponding ¹³C NMR spectrum also supported the structure of DPA-PEPA-Boz. The two singlets at 115.8 ppm and 57.7 ppm were the typical carbon resonances of -N-CH₂-O- and -N-CH₂-Ph- of the oxazine ring respectively. No detectable resonances due to impurities were seen in the spectrum.

With the same methods the other synthesized monomers were characterized by means of these spectra, and the results were given in the Experimental Section.

3.2. Curing behavior of DPA-Boz, MDP-Boz and DPA-PEPA-Boz

1,3-benzoxazines exhibit exothermic ring-opening reaction in the condition of heating and/or the existence of catalyst, which can be observed by DSC [36]. DSC was carried out to study curing behavior of DPA-Boz, MDP-Boz and DPA-PEPA-Boz. Fig. 5 showed the typical nonisothermal DSC thermograms, and the results were summarized in Table 2.

The DSC curve given in Fig. 5 showed a clear one-stage curing for MDP-Boz, with a sharp exothermic peak in a temperature range of 166–280 °C and the maximum at 230.6 °C (T_{max}). The DSC curve of DPA-Boz also showed a broad one-stage curing with a temperature range of 150–270 °C, but shifted to a lower temperature with the peak temperature (T_{max}) changing from 230.6 °C to 189.2 °C due to the presence of carboxyl group in DPA-Boz. Its ΔH value also decreased from 353.9 J/g to 323.7 J/g. It is well known that proton acid is a common catalyst of Boz [37], and the carboxyl in DPA-Boz played a catalytic role leading to the exothermic ring-opening reaction shifting to a lower temperature. In contrast to MDP-Boz and DPA-Boz monomers, the DSC curve of DPA-PEPA-Boz showed a two-stage curing with two maximums at 221.7 °C and 272.0 °C respectively. The first exothermic peak was the exothermic reactions of the oxazine-ring opening, with a temperature range of 159.3–257.3 °C and the maximum at 221.7 °C (T_{max1}). The second exothermic peak was the -P-O-C- ring opening in PEPA, with an exothermic peak in a temperature range of 257.3–293.7 °C and the maximum at 272.0 °C [37]. The temperature range of the exothermic curing peak of DPA-PEPA-Boz was close to that of MDP-Boz and about 30 °C higher than that of DPA-Boz. This was mainly because there was no proton acid in the structure of DPA-PEPA-Boz due to the introduction of PEPA.

3.3. Thermal properties of the cured benzoxazine resins

The thermal and thermal-oxidative decompositions of cured Bozs (denoted as P-) were evaluated by using TG under nitrogen and air atmospheres. The TG curves of cured Bozs and their derivatives (DTG) were shown in Figs. 6 and 7, and the results were summarized in Tables 3 and 4. $T_{5\%}$, $T_{10\%}$ and $T_{50\%}$ were the temperatures for 5%, 10% and 50% mass losses, respectively. $T_{5\%}$ is defined as the onset temperature of the degradation of the cured Bozs. T_{max} is the temperature with the maximum mass loss rate. Peak value is the maximum mass loss rate during the decomposition. Char is the percentage of the char yielded at 800 °C under

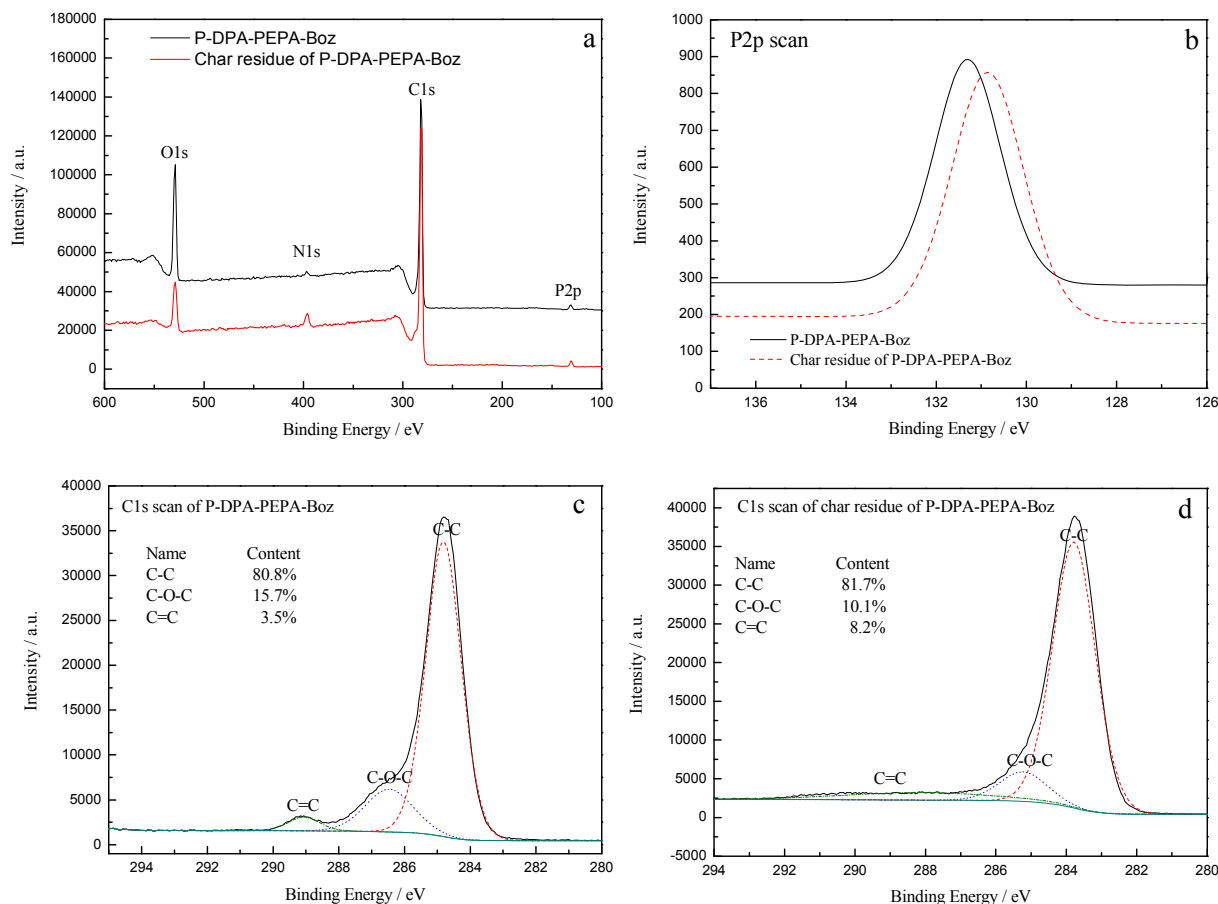


Fig. 8. XPS survey scan (A), P2p (B), C1s ((C) and (D)) scan of P-DPA-PEPA-Boz and its char residue.

Table 5

Element content of P-DPA-PEPA-Boz and its char residue determined by XPS.

Elements (at. %)	C	N	O	P
P-DPA-PEPA-Boz	63.94	2.40	31.54	2.12
Residue of P-DPA-PEPA-Boz	83.80	3.66	10.12	2.42

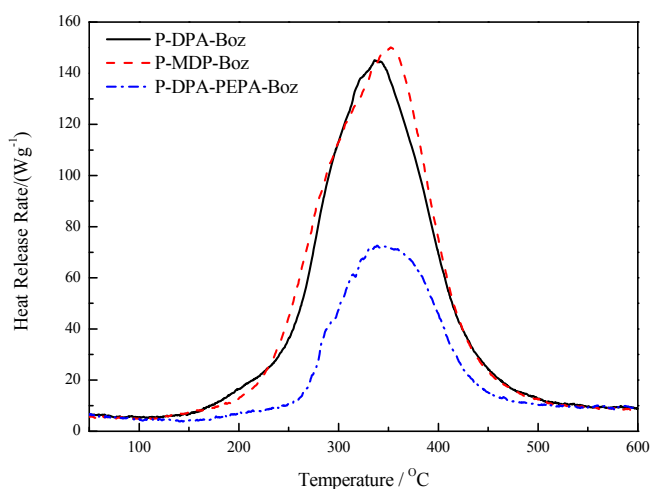


Fig. 9. MCC curves of the cured benzoxazine resins from DPA-Boz, MDP-Boz and DPA-PEPA-Boz.

nitrogen, and $T_{Char=0}$ is the temperature with no char residue under air atmosphere.

As shown in Fig. 6 and Table 3, $T_5\%$, $T_{10\%}$ and T_{max} of P-DPA-Boz were 343.6, 376.6 and 442.2 °C respectively, and the residual char at 800 °C was 37.9%. P-DPA-Boz showed good thermal stability. In its DTG curve, P-DPA-Boz showed a one-stage weight loss process with its peak value at 8.64 wt%/min. Compared to P-DPA-Boz, thermal stability of P-MDP-Boz was slightly weakened with the lower values of $T_5\%$, $T_{10\%}$, $T_{50\%}$ and the residual char. This was mainly because the methyl group introduced in the structure of P-MDP-Boz was more readily to be decomposed. As for P-DPA-PEPA-Boz, its $T_5\%$ was 341.5 °C, slight lower than that of P-DPA-Boz. This was because PEPA first decomposed at about 300 °C during the decomposition process. PEPA is a highly effective flame retardant, and can form an insulating layer to cover the resin surface after decomposition, which isolates air and hinders further combustion of resins [38]. As the results, the residual char of P-DPA-PEPA-Boz (55.4%) was much higher than that of P-DPA-Boz (37.4%) and P-MDP-Boz (32.5%) at 800 °C. From the DTG results, the mass loss rate of P-DPA-PEPA-Boz was the lowest under the same temperature due to the existence of PEPA in the molecular structure, whereas that of P-MDP-Boz was the highest because methyl group promoted decomposition of the carbon sources. Peak value of P-DPA-PEPA-Boz was 4.50 wt%/min, which was only 52.09% of P-DPA-Boz (8.64 wt%/min) and 51.20% of P-MDP-Boz (8.79 wt%/min). $T_{50\%}$ is another parameter to effectively evaluate thermal stability of polymer. $T_{50\%}$ of P-DPA-PEPA-Boz was higher than 950 °C while that of P-DPA-Boz and P-MDP-Boz were only 498.4 °C and 482.8 °C respectively. The results revealed that the introduction of PEPA in

Table 6
MCC results of the cured benzoxazine resins from DPA-Boz, MDP-Boz and DPA-PEPA-Boz.

Sample	HRC J/g.K	HRC* J/g.K	PHRR w/g	THR kJ/g	T _{PHRR} °C
P-DPA-Boz	139 ± 2	227	127.3 ± 1.8	18.3 ± 0.2	424.4 ± 0.3
P-MDP-Boz	146 ± 1	249	114.2 ± 1.6	19.4 ± 0.1	408.8 ± 0.9
P-DPA-PEPA-Boz	68 ± 1	188	55.4 ± 1.1	8.6 ± 0.1	417.2 ± 0.2

HRC* was calculated for bio-based Bozs from their chemical structures by Ref. [39].

Table 7
Flame retardant properties of the cured benzoxazine resins from DPA-Boz, MDP-Boz and DPA-PEPA-Boz.

Sample	LOI (%)	Vertical burning tests		
		t ₁ (s)	t ₂ (s)	UL-94 rate
P-DPA-Boz	26.1	Fail	Fail	No rating
P-MDP-Boz	25.7	Fail	Fail	No rating
P-DPA-PEPA-Boz	33.5	1.68	0.12	V-0

the structure of bio-based boz could enhance effectively the control of thermal transmission and at the same time form the protective intumescent char layer on the surface during thermal degradation.

The TG curves of the cured Bozs under air atmosphere were shown in Fig. 7. The results also showed that P-DPA-PEPA-Boz had much better thermal-oxidative stability than other two resins. P-DPA-Boz and P-MDP-Boz had a similar decomposition behavior with a distinct two-step decomposition process. As shown in Table 4, $T_5\%$, $T_{10\%}$, T_{max1} , T_{max2} of P-DPA-Boz were 360.3, 400.3, 437.1 and 656.0 °C respectively, and the no residual char temperature was about 750 °C. In its DTG curve, the peak value₁ and peak value₂ were 5.46 and 7.78 wt%/min respectively. The results for P-MDP-Boz were similar and slightly lower because of the methyl group. However, the P-DPA-PEPA-Boz decomposition occurred very differently in a distinct four-step process and there was still 10.5% of the residual char at 900 °C. Its T_{max} s were 467.0, 569.0, 650.0 and 744.0 °C respectively and peak values were 3.73, 4.20, 4.54 and 3.20 wt%/min respectively. Its residual char at temperatures ranging from 400 to 950 °C was significantly higher than those of P-DPA-Boz and P-MDP-Boz. These results indicated the lower mass loss rate and much more efficient char formation during thermal-oxidation decomposition of P-DPA-PEPA-Boz. The literature suggested that the second decomposition step was mostly ascribed to the oxidation degradation of the char layer and the following release of CO and CO₂ [22]. Therefore, the higher thermal oxidation stability in the second stage was most likely due to the formation of thick and dense stable intumescent chars in the first stage, which could efficiently hinder the oxygen permeability and the simultaneous thermal transmission. Thus, PEPA acted as intrinsic flame retardant and produced remarkable effects on the thermal-oxidative decomposition of the cured Boz under air environment.

The XPS spectra of P-DPA-PEPA-Boz and its char residue were shown in Fig. 8, and their element contents were summarized in Table 5. The surface content of phosphorus was also increased slightly from 2.12 wt% to 2.42 wt%, while the surface content of oxygen was decreased from 31.54 wt% to 10.12 wt%. Obviously, the surface content of carbon was increased from 63.94 wt% to 83.80 wt% and the surface content of C—C and C=C of char residue was higher than those of P-DPA-PEPA-Boz, revealing that PEPA endowed P-DPA-PEPA-Boz good char-forming ability and then P-

DPA-PEPA-Boz had excellent thermal stability.

3.4. Combustion properties and flame retardancy of the cured benzoxazine resins

In order to further analyze the correlation between the cross-linked structure and flammability for cured Bozs, their aerobic pyrolysis and the subsequent reactions between the volatile pyrolysis products and a mixture of nitrogen/oxygen (80/20) gas under high temperatures were simulated by microscale combustibility calorimeter experiments. The key combustion parameters, including heat release capacity (HRC), total heat release (THR), peak heat release rate (PHRR) and the temperature for the PHRR (T_{PHRR}), were obtained. The representative heat release rate curves of the cured Bozs were presented in Fig. 9, and the detailed data were summarized in Table 6.

As shown in Fig. 9 and Table 6, all three Bozs had one wide overlapping exothermic peak from 50 to 600 °C in the MCC curve. The THR, HRC and PHRR of P-DPA-Boz and P-MDP-Boz were similar at about were 19 kJ/g, 140 J/g.K and 120 w/g respectively. However, the results of P-DPA-PEPA-Boz were much lower, only half of that of P-DPA-Boz and P-MDP-Boz, at 8.6 kJ/g, 55.4 w/g and 68 J/g.K respectively. As shown in Table 6, the changes of HRC values for these bio-based bozs were consistent with those calculated for bio-based bozs according to their chemical structures [39]. The introduction of PEPA flame retardant moiety, which was decomposed to produce a layer of char layer at 300 °C, significantly improved the flame retardancy of the materials. The results indicated that PEPA was an excellent intrinsic flame retardant for the cured Bozs and could effectively retard their combustion, reduce their combustion speed, burning degree and combustion heat release.

The flame retardant property of the cured Bozs was also assessed by the LOI and the vertical flame tests, as shown in Table 7. The LOI values of the P-DPA-Boz and P-MDP-Boz were only 26.1% and 25.7% respectively. P-DPA-Boz and P-MDP-Boz showed no rating in UL94 test. For the P-DPA-PEPA-Boz, LOI value was even higher, at 33.5%. Its t_1 and t_2 were 1.68 and 0.12 s respectively, which were significantly lower than the maximum permissible values of 10 s, indicated in flame retardancy standards. P-DPA-PEPA-Boz achieved V0 rating in UL94 test. LOI values of the bio-based Bozs from eugenol [40,41] and phosphorus flame retardant P-DPA-Bozs [27] were shown in Table 8. As shown in Table 8, LOI value of P-DPA-PEPA-Boz was higher than those of the bio-based bozs from eugenol except F-BZ and almost same as those of DOPO flame retardant P-DPA-Boz. Therefore, P-DPA-PEPA-Boz behaved as a very good intrinsic flame retardant bio-based Boz.

4. Conclusions

In this study, an intrinsically flame retardant bio-based boz

Table 8
LOI values of the bio-based Bozs from eugenol) and phosphorus flame retardant P-DPA-Bozs [27,40,41].

Boz	S-Bz	F-Bz	Bz-OXY	Bz-PHE	Bz-DDS	Bz-SUL	Phosphorus flame retardant P-DPA-Bozs
LOI (%)	27.1	39.0	29.4	32.1	30.3	26.9	31.6–35.4

(DPA-PEPA-Boz) had been synthesized and characterized. The DSC curve of DPA-PEPA-Boz monomer showed a two-stage curing with two maximums at 221.7 °C and 272.0 °C, assigned to the exothermic opening reactions of oxazine rings and -P-O-C ring in PEPA, and its exothermic curing peak was close to that of MDP-Boz monomer and about 30 °C higher than that of DPA-Boz monomer. Compared with P-DPA-Boz and P-MPA-Boz, $T_{5\%}$ of P-DPA-PEPA-Boz was slightly lower. However, its residual char after 400 °C was higher, especially under nitrogen atmosphere. The THR, PHRR and HRC of P-DPA-PEPA-Boz were less than half of those of P-DPA-Boz and P-MDP-Boz. P-DPA-PEPA-Boz achieved a significantly high LOI value at 33.5% and VO rating in the UL94 test. Therefore, P-DPA-PEPA-Boz behaved as a very good intrinsic thermal stable and flame retardant bio-based Boz.

Acknowledgements

We gratefully acknowledge the financial supports from the National Natural Science Foundation of China (No. 51103129), Zhejiang Provincial Natural Science Foundation of China (No. LY14E030006), Ningbo Science and Technology Innovation Team (No. 2015B11005), and Ningbo Natural Science Foundation (No.2015A610028).

References

- [1] A. Gandini, *Macromolecules* 41 (2008) 9491–9504.
- [2] M.N. Belgacem, A. Gandini, , *Monomers, Polymers and Composites from Renewable Resources*, Elsevier, Oxford, 2008.
- [3] C. Li, X.Q. Liu, J. Zhu, C.Z. Zhang, J.S. Guo, *J. Macromol. Sci. A* 50 (2013) 321–329.
- [4] S.Q. Ma, X.Q. Liu, Y.H. Jiang, Z.B. Tang, C.Z. Zhang, J. Zhu, *Green Chem.* 15 (2013) 245–254.
- [5] Q.Q. Ma, X.Q. Liu, R.Y. Zhang, J. Zhu, Y.H. Jiang, *Green Chem.* 15 (2013) 1300–1310.
- [6] J.Y. Dai, S.Q. Ma, Y.G. Wu, L.J. Han, L.S. Zhang, J. Zhu, X.Q. Liu, *Green Chem.* 7 (2015) 2383–2392.
- [7] C. Zúñiga, G. Lligadas, J.C. Ronda, M. Galià, V. Cádiz, *Polymer* 53 (2012) 1617–1623.
- [8] F. Carosio, J. Kochumalayil, F. Cuttica, G. Camino, L. Berglund, *ACS Appl. Mater. Interfaces* 7 (2015) 5847–5856.
- [9] J.X. Feng, X.M. Zhang, S.Q. Ma, Z. Xiong, C.Z. Zhang, Y.H. Jiang, J. Zhu, *Ind. Eng. Chem. Res.* 52 (2013) 2784–2792.
- [10] Y. Liu, Y. Zhang, Z.P. Fang, *BioResources* 7 (2012) 4914–4925.
- [11] N.N. Ghosh, B. Kiskan, Y. Yagci, *Prog. Polym. Sci.* 32 (2007) 1344–1391.
- [12] A. Chernykh, T. Agag, H. Ishida, *Polymer* 50 (2009) 382–390.
- [13] K.W. Huang, S.W. Kuo, *Macromol. Chem. Phys.* 211 (2010) 2301–2311.
- [14] R. Andreu, M.A. Espinosa, M. Galià, V. Cádiz, J.C. Ronda, J.A. Reina, *J. Polym. Sci. Part A Polym. Chem.* 44 (2006) 1529–1540.
- [15] Y.F. Zhu, Y. Gu, *J. Macromol. Sci. Part B Phys.* 50 (2011) 1130–1143.
- [16] A. Chernykh, J. Liu, H. Ishida, *Polymer* 47 (2006) 7664–7669.
- [17] T. Zhang, H.Q. Yan, Z.P. Fang, M. Peng, *Chin. J. Polym. Sci.* 31 (2013) 1359–1371.
- [18] H.Q. Yan, H.Q. Wang, J. Cheng, Z.P. Fang, *RSC Adv.* 5 (2015), 18538–15545.
- [19] H.Q. Yan, H.Q. Wang, Z.P. Fang, *Ind. Eng. Chem. Res.* 53 (2014) 19961–19969.
- [20] T.T. Feng, J. Wang, H. Wang, N. Ramdani, L.W. Zu, W.B. Liu, X. Xu, *Polym. Adv. Technol.* 26 (2015) 581–588.
- [21] J.Y. Cha, M.A. Hanna, *Ind. Crop. Prod.* 16 (2002) 109–118.
- [22] M.Y. Chen, M. Ike, M. Fujita, *Environ. Toxicol.* 17 (2002) 80–86.
- [23] K.H. Kim, J.Y. Moon, D.H. Ha, D.W. Park, *React. Kinet. Catal. Lett.* 75 (2002) 385–395.
- [24] P. Zhang, L.B. Wu, B.G. Li, *Polym. Degrad. Stabil.* 94 (2009) 1261–1266.
- [25] G. Lligadas, A. Tüzün, J.C. Ronda, M. Galià, V. Cádiz, *Polym. Chem.* 5 (2014) 6636–6644.
- [26] C. Zúñiga, L. Bonnaud, G. Lligadas, J.C. Ronda, M. Galià, V. Cádiz, P. Dubois, *J. Mater. Chem. A* 2 (2014) 6814–6822.
- [27] C. Zúñiga, M.S. Larrechi, G. Lligadas, J.C. Ronda, M. Galià, V. Cádiz, *Polym. Degrad. Stabil.* 98 (2013) 2617–2626.
- [28] C.W. Chang, C.H. Lin, H.T. Lin, H.J. Huang, K.Y. Hwang, A.P. Tu, *Eur. Polym. J.* 45 (2009) 680–689.
- [29] G.M. Yu, L.S. Wang, C.J. Du, *J. Chem. Eng. Data* 59 (2014) 1454–1460.
- [30] C.X. Lu, T. Chen, X.F. Cai, *J. Macromol. Sci. Part B Phys.* 48 (2009) 651–662.
- [31] V. Sarannya, P. Sivasamy, N.D. Mathan, R. Tajkumar, C.T. Vijayakumar, D. Ponraju, *J. Therm. Anal. Calorim.* 102 (2010) 1071–1077.
- [32] M.P. Luda, A.I. Balabanovich, M. Zanetti, D. Guaratto, *Polym. Degrad. Stab.* 92 (2007) 1088–1100.
- [33] W.C. Zhang, X.D. He, T.L. Song, Q.J. Jiao, R.J. Yang, *Polym. Degrad. Stab.* 109 (SI) (2014) 209–217.
- [34] Z. Brunovska, J.P. Liu, H. Ishida, *Macromol. Chem. Phys.* 200 (1999) 1745–1752.
- [35] C. Zúñiga, M.S. Larrechi, G. Lligadas, J.C. Ronda, M. Galià, V. Cádiz, *J. Polym. Sci. Part A Polym. Chem.* 49 (2011) 1219–1227.
- [36] Q.C. Ran, D.X. Zhang, R.Q. Zhu, Y. Gu, *Polymer* 53 (2012) 4119–4127.
- [37] N.D. Mathan, T. Rajkumar, C.T. Vijayakumar, M. Arunjunairaj, D. Ponraju, *J. Therm. Anal. Calorim.* 110 (2012) 1133–1141.
- [38] W. Zhao, J.P. Liu, H. Peng, J.Y. Liao, X.J. Wang, *Polym. Degrad. Stab.* 118 (2015) 120–129.
- [39] R.N. Walters, R.E. Lyon, *J. Appl. Polym. Sci.* 87 (2003) 548–563.
- [40] P. Thirukumar, A. Shakila, M. Sarojadevi, *RSC Adv.* 4 (2015) 7959–7966.
- [41] P. Thirukumar, A. Shakila Parveen, M. Sarojadevi, *ACS Sustain. Chem. Eng.* 2 (2014) 2790–2801.